Structural selection of graphene supramolecular assembly oriented by molecular conformation and alkyl chain

Qing Chen[a,b], Ting Chen[a,b], Ge-Bo Pan[a], Hui-Juan Yan[a], Wei-Guo Song[a], Li-Jun Wan[a,1], Zhong-Tao Li[a,b], Zhao-Hui Wang[a], Bo Shang[c], Lan-Feng Yuan[c], and Jin-Long Yang[c]

[a]Institute of Chemistry and [b]Graduate School of the Chinese Academy of Sciences, Chinese Academy of Sciences, Beijing 100190, China and Beijing National Laboratory for Molecular Sciences, Beijing 100190, China; [c]Hefei National Laboratory for Physical Sciences at Microscale, University of Science and Technology of China, Hefei, Anhui 230026, China

Communicated by Chunli Bai, Chinese Academy of Sciences, Beijing, People's Republic of China, September 19, 2008 (received for review June 1, 2008)

Graphene molecules, hexafluorotribenzo[a,g,m]coronene with *n*-carbon alkyl chains (FTBC-Cn, *n* = 4, 6, 8, 12) and Janus-type "double-concave" conformation, are used to fabricate self-assembly on highly oriented pyrolytic graphite surface. The structural dependence of the self-assemblies with molecular conformation and alkyl chain is investigated by scanning tunneling microscopy and density functional theory calculation. An interesting reverse face "up–down" way is observed in FTBC-C4 assembly due to the existence of hydrogen bonds. With the increase of the alkyl chain length and consequently stronger van der Waals interaction, the molecules no longer take alternating "up–down" orientation in their self-assembly and organize into various adlayers with lamellar, hexagonal honeycomb, and pseudohoneycomb structures based on the balance between intermolecular and molecule-substrate interactions. The results demonstrate that the featured "double-concave" molecules are available block for designing graphene nanopattern. From the results of scanning tunneling spectroscopy measurement, it is found that the electronic property of the featured graphene molecules is preserved when they are adsorbed on solid surface.

graphene molecule | Janus-type double-concave conformation | scanning tunneling microscopy | self-assembly

A graphene molecules is composed of fused aromatic sets and is regarded as graphite subunit. After the success in theoretical prediction and experimental realization of graphene, graphene type molecules attract a great deal of interest (1–4). Their unique structures provide them promising potentials in micro/nano electronic devices (5–7). Continuous effort in chemical synthesis of graphene type molecules has produced various graphene molecules with the structures and properties beyond simple graphene. For example, polycyclic aromatic hydrocarbons (PAHs) compounds belong to a class of important functional graphene molecules (7, 8). PAHs and their derivatives contain 2D subsections of graphene and show significant advantages, such as good solubility and ability to bear different chemical functionalities in their periphery with various electronic properties. These graphene molecules are promising candidates as building block for nanodevices through self-assembled architectures on 2D solid surfaces (9, 10).

As a powerful tool for nanoscience and nanotechnology, scanning probe microscopy, in particular, scanning tunneling microscopy (STM) studies have produced images of the molecular self-assembly of graphene molecules at atomic/submolecular resolution, providing molecular understanding of intermolecular interactions and origin of their physical/chemical properties (11–14). Because of their chemical structures, most of PAHs have a planar conformation and are inclined to form well-defined long-range self-assemblies on various substrates, such as gold and highly oriented pyrolytic graphite (HOPG). For examples, an alkyl-substituted PAH with D_{2h} symmetry and 78 carbon atoms in the aromatic core can self-assembly on HOPG surface, and exhibit a diode-like current versus voltage feature by STM (15). And hexa-*peri*-hexabenzocoronene was found to self-organize into ordered adlayer on HOPG surface, and its aromatic moieties were oriented like a graphene layer in graphite (16–18).

Recently, an intriguing class of curved PAHs molecules was synthesized. Their aromatic rings are contorted to adopt an unusual intermolecular arrangement during self-assembly (19–22). In particular, the curved PAHs with Janus-type double-concave conformation, where one face of the molecule is different from the other, exhibits novel properties induced by phase separation of their faces (23). However, molecular understanding of the assembly of such nonplanar Janus-type double-concave curved PAHs is lacking. Preparing and understanding the self-assembly of these graphene molecules remain a challenging subject in surface science, chemistry, and nanotechnology and is an important preliminary step in developing graphene based nanodevices.

In this work, a new series of Janus-type double-concave graphene molecules, hexafluorotribenzo[a,g,m]coronene with different *n*-carbon alkyl chains (FTBC-Cn, *n* = 4, 6, 8, 12) was designed and synthesized. The chemical structure of FTBC-Cn is illustrated in Fig. 1. They are triangle-shaped molecules with 2 alkyl chains at the midpoints of each side (24). The molecules show different conformation in their crystals. For example, steric congestion in the bay regions induces a unique conformation with the likelihood of 2 different concave faces and molecules assemble as dimer in FTBC-C4 crystal (25). However, on a solid substrate the molecule-substrate interaction and intermolecular interaction will influence the adsorption structure of these molecules, leading to different molecular conformations and adlayer structures.

We studied the self-assemblies of these molecules on HOPG surface using STM. The effect of the nonplanar polycyclic aromatic cores and alkyl chains of different lengths on 2D self-assembly at ambient conditions is investigated. The results show that all molecules form ordered monolayers on HOPG surface. The molecular conformation and alkyl chain dominate the assembly structure. An alternating upward and downward (up–down) molecular orientation order is observed in the self-assembly of FTBC-C4. When the alkyl chain length is increased, the ordered face reverse up–down appearance dis-

Author contributions: L.-J.W. designed research; Q.C. and B.S. performed research; Z.-T.L. and Z.-H.W. contributed new reagents/analytic tools; Q.C., T.C., G.-B.P., H.-J.Y., L.-J.W., B.S., L.-F.Y., and J.-L.Y. analyzed data; and Q.C., W.-G.S., L.-J.W., and L.-F.Y. wrote the paper.

The authors declare no conflict of interest.

[1]To whom correspondence should be addressed. E-mail: wanlijun@iccas.ac.cn.

This article contains supporting information online at www.pnas.org/cgi/content/full/0809427105/DCSupplemental.

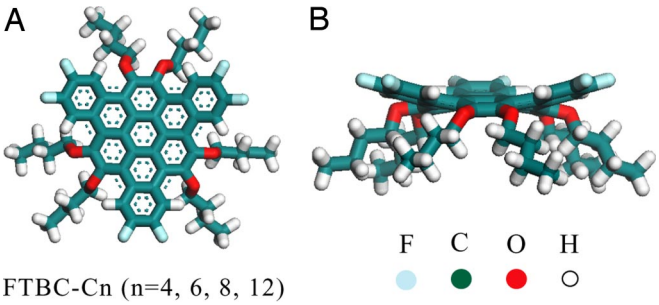

Fig. 1. The chemical structure of FTBC-Cn. Top view (*A*) and side view (*B*) with *n*-carbon alkyl side chains (n = 4, 6, 8, 12) optimized by DFT. The side alkyl chains represented in this figure is butyls.

appears, and various ordered adlayers with lamellar, hexagonal honeycomb, and pseudohoneycomb structures are formed. Furthermore, the electronic properties of these molecules are studied by scanning tunneling spectroscopy (STS).

Results

FTBC-C4 Assembly. Fig. 2*A* is a typical large-scale STM image acquired on FTBC-C4 adlayer on HOPG surface. The FTBC-C4 molecule adsorbs on HOPG surface and self-organizes into well-ordered adlayer. The adlayer with regular molecular rows extends to >100 nm. Fig. 2*B* is a high-resolution STM image showing the details of the self-assembly. The molecular rows are composed of individual molecules. The main feature in a single molecule is a set of 3 bright spots in a triangular shape, consistent with the calculated lowest unoccupied molecular orbital (LUMO) of FTBC-C4 shown in Fig. 2*B Inset*. The side length of the triangular shape is measured to be 1.3 ± 0.1 nm, which is consistent with the calculated value of a FTBC-Cn molecule in Fig. 2*B Inset*. The triangle-shaped parts are thus ascribed to the polycyclic aromatic π-conjugated molecular cores of the FTBC-C4 molecule. The alkyl chains are not resolved by STM imaging in this observation because shorter C4 chains are not firmly adsorbed on HOPG surface and retain high degrees of conformational freedom (26). Moreover, the alkyl chains usually exhibit lower tunneling probability than the conjugated graphene cores.

Intriguingly, the self-assembly consists of 2 alternating molecular rows as indicated by arrows A and B in Fig. 2*B*. The molecules in row A appear in bright contrast, whereas in row B they appear in dark contrast. The alternating bright and dark rows propagate throughout the whole adlayer. Li *et al.* (25) reported that the 3D crystal of the FTBC-C4 molecular core is markedly nonplanar due to pronounced peri-interactions. X-ray diffraction results indicate that a Janus-type "double-concave" conformation is formed, consisting of a curved π-conjugated core and a plate-shaped hollow by side chains. Therefore, FTBC-C4 molecules can take 2 different orientations on HOPG surfaces, i.e., "down" (alkyl chains in contact with HOPG) and "up" conformation (conjugated core in contact with substrate). The existence of 2 types of contrasts in STM images indicates that 2 opposite orientations, "up" and "down," respectively, are taken by FTCB-C4 molecules as shown in Fig. 2*B*. According to the molecular periodicity and adlayer symmetry, a rectangular unit cell is determined as outlined in Fig. 2*B*. Four bright molecules are positioned on the corners with a dark molecule in the center. The unit cell constants are determined from the STM image to be a = 2.62 ± 0.1 nm and b = 2.12 ± 0.1 nm.

Density functional theory (DFT) calculations indicate that the "down" orientation present higher electronic state density than the "up" one (see *Discussion*). Therefore, the bright triangle in STM image should be from the "down" orientation, in which the

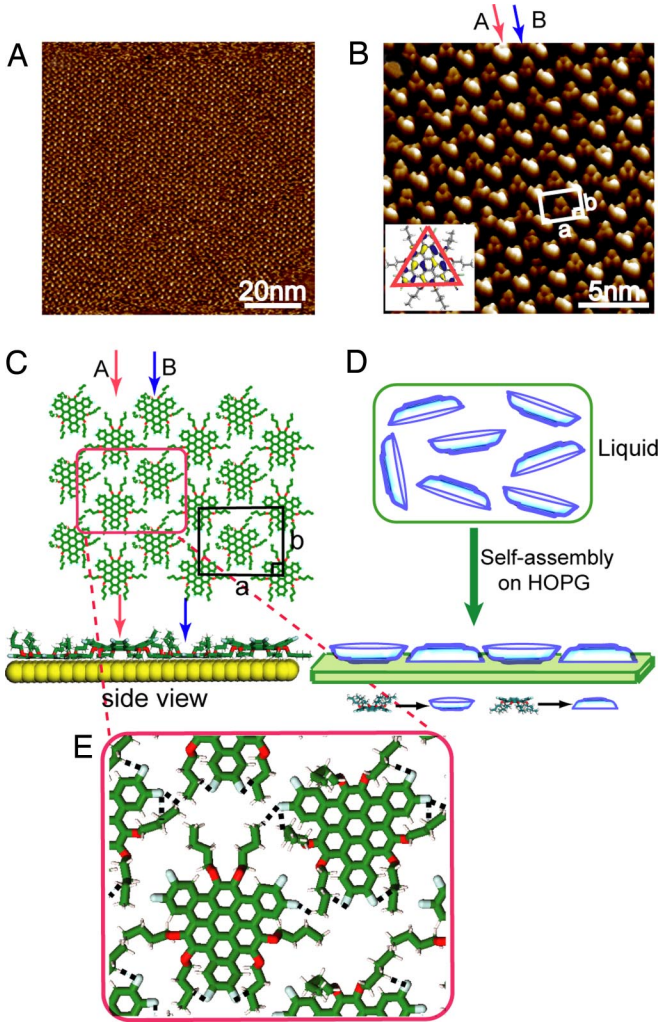

Fig. 2. Self-assembly of FTBC-C4 on HOPG. (*A*) Large-scale STM image. V_{bias} = 650 mV; I_t = 670 pA. (*B*) High-resolution STM image. V_{bias} = 753 mV; I_t = 674 pA. (*Inset*) Calculated LUMO of an FTBC-C4 molecule. The arrow A and B in red and blue indicate the "down" and "up" conformation, respectively. (*C*) Top and side views of the proposed structural model for the ordered FTBC-C4 adlayer. (*D*) Schematic illustration of "up–down plates" represents the molecular orientation in the self-assembly. (*E*) Possible hydrogen bonds indicated by black dashed lines.

vertex of triangle corresponds to the π-conjugated core. In contrast, the vertex of triangle is ascribed to the O atoms of alkyl chains in the "up" orientation. Moreover, the bright and dark triangles pack in a "vertex to vertex" configuration. F atoms in the "down" oriented molecules face the alkyl chains of the "up" oriented molecules. Therefore, it is deduced that in row A the molecules take "down" orientation and result in bright contrast, whereas the molecules in row B take "up" orientation in dark contrast. On the basis of the calculations, the structural model for the ordered adlayer is proposed in Fig. 2*C*. A schematic illustration of the self-assembly is given in Fig. 2*D*. The curved FTBC-C4 molecules depicted as "plates" are initially dispersed randomly in toluene solution. When the molecules are self-assembled on HOPG, the "plates" self-organize into an ordered assembly with an "up–down" arrangement. Fig. 2*E* shows the possible intermolecular and intramolecular C–H···F hydrogen bonds in the assembly, which play important roles in forming the assembly.

FTBC-C6 Assembly. FTBC-C6 molecules form well-defined adlayer on HOPG. Fig. 3*A* is a large-scale STM image showing the

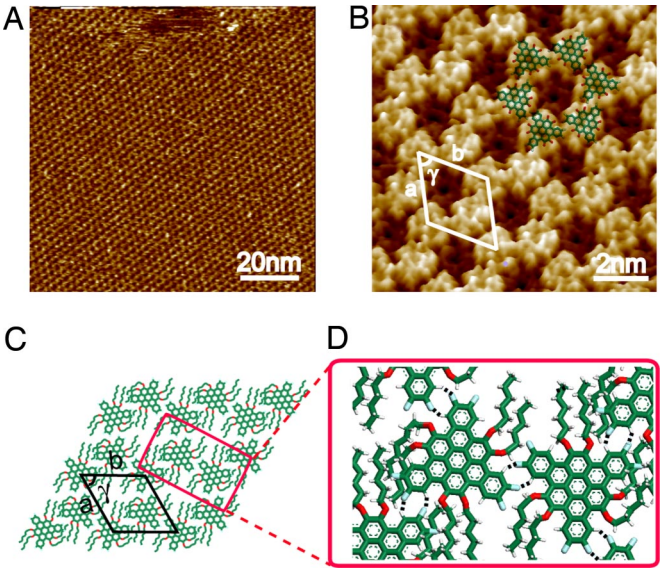

Fig. 3. Self-assembly of FTBC-C6 on HOPG. (*A*) Large-scale STM image. V_{bias} = 1.28 V; I_t = 420 pA. (*B*) High-resolution STM image. V_{bias} = 1.06 V; I_t = 223 pA. (*C*) Proposed structural model for the ordered adlayer. (*D*) Possible hydrogen bonds between the molecules indicated by black dashed lines.

ordered self-assembled molecular nanostructure. However, the increase of 2 more methylenes in the alkyl substituents made the self-assembly of FTBC-C6 drastically different from that of FTBC-C4, as shown in high-resolution STM image in Fig. 3*B*. The alternating bright and dark rows in FTBC-C4 adlayer (Fig. 2*B*) disappear in FTBC-C6 assembly, instead a honeycomb structure forms. Each honeycomb unit is composed of 6 bright spots with a dark depression at the center. A careful examination found that each bright spot corresponds to a FTBC-C6 molecule, and the molecules in a honeycomb unit form a close packed assembly. The molecular models are depicted and superimposed on the image. An image contrast can be seen in the depression area and is ascribed to alkyl chains. However, the structural details of the alkyl chains are not well resolved because of relative short chain.

The molecules shown in Fig. 3*B* take the same adsorption orientation on HOPG surface. A rhombic unit cell is defined and outlined in Fig. 3*B*. The lattice constants were determined to be $a = b = 2.60 \pm 0.1$ nm, and $\gamma = 60 \pm 2°$. Fig. 3*C* is a tentative structural model for the ordered structure of FTBC-C6 deduced from the high-resolution STM image in Fig. 3*B*. In this model, the molecules self-organize into honeycomb structure on HOPG surface with the same flat-lying orientation. The C–H···F hydrogen bond (marked by black dashed lines in Fig. 3*D*) plays an essential role in forming the honeycomb network. To simplify the model, the alkyl chains are arranged as in the model, but other conformations, such as overlapping or reaching out of the HOPG surface are possible.

FTBC-C8 Assembly. Similar to FTBC-C6, FTBC-C8 molecules also form hexagonal honeycomb network. As shown in supporting information (SI) Fig. S1 *a* and *b*. The lattice constants were determined to be $a = b = 2.70 \pm 0.1$ nm, and $\gamma = 60 \pm 2°$.

FTBC-C12 Assembly. With increase of the alkyl chain length to 12 carbons, van der Waals interaction will play an important role in the self-assembly formation. The other important interaction is the π–π interaction between polycyclic aromatic cores of the graphene molecules and HOPG substrate. These interactions result in 2 structures, lamellar and pseudohoneycomb structures.

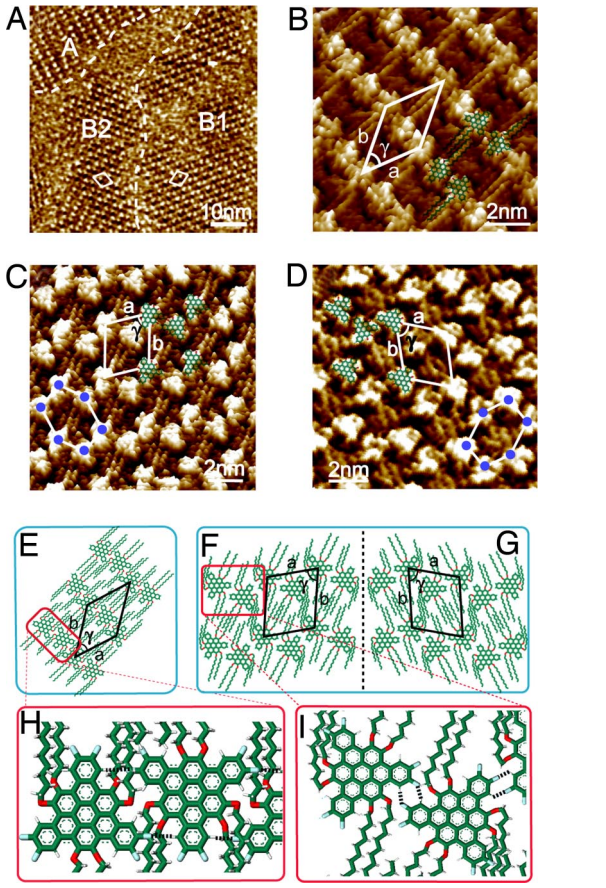

Fig. 4. Self-assembly of FTBC-C12 on HOPG. (*A*) Large-scale STM image showing both lamellar and pseudohoneycomb structures denoted as A and B. B1 and B2 are 2 mirror-symmetric domains. The boundaries are marked by white dashed lines. V_{bias} = 984 mV; I_t = 503 pA. (*B*) High-resolution STM image of domain A (lamellar structure). V_{bias} = 850 mV; I_t = 410 pA. (*C* and *D*) High-resolution STM images of domains B1 (*C*) and B2 (*D*) (pseudohoneycomb structure). A chiral adlayer is corresponded between the 2 domains. (*C*) V_{bias} = 880 mV; I_t = 500 pA. (*D*) V_{bias} = 850 mV; I_t = 498 pA. (*E*–*G*) Structural models for the ordered adlayers of A, B1, and B2. In *F* and *G*, the structural models show the mirror symmetry in B1 and B2. (*H* and *I*) Possible hydrogen bonds between the neighboring molecules indicated by black dashed lines in lamellar and pseudohoneycomb structures, respectively.

Fig. 4*A* shows a typical large-scale STM image of FTBC-C12 adlayer on HOPG surface. Three ordered domains are observed, indicated by A, B1 and B2, respectively. The domain boundary is illustrated by white dashed line. Intriguingly, B1 and B2 domains are mirror-symmetric.

Lamellar Structure. Fig. 4*B* shows a high-resolution STM image acquired in domain A. FTBC-C12 molecules form ordered rows with a typical lamellar appearance, and van der Waals interaction between the neighboring alkyl chains is important in forming the molecular assembly. The bright spots are ascribed to the polycyclic aromatic graphene cores. The dark troughs are due to the alkyl chains. These alkyl chains interdigitate each other between different lamellas, resulting in a close-packed molecular assembly. The molecules in a lamella take opposite directions between the neighboring molecules as illustrated in the superimposed molecular models of Fig. 4*B*. On the basis of the adlayer symmetry and molecular arrangement, a unit cell is outlined in Fig. 4*B*. The lattice constants were measured to be $a = 2.78 \pm 0.1$ nm, $b = 3.20 \pm 0.1$ nm, and $\gamma = 45 \pm 2°$. A tentative structural model is presented in Fig. 4*E*. The details from theoretical calculation are shown in the model of Fig. 4*H*.

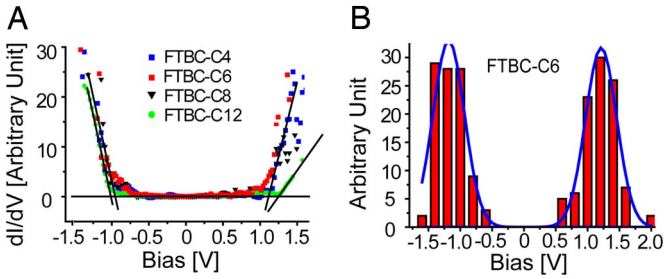

Fig. 5. STS results of FTBC-Cn (n = 4, 6, 8, 12). (*A*) Typical dI/dV-V curves obtained on FTBC-Cn adlayers on HOPG in ambient condition. (*B*) The histogram of experimental gap edges of FTBC-C6. The blue solid lines show a Gauss fit of the columns.

Pseudohoneycomb Structure. Fig. 4 *C* and *D* are high-resolution STM images from domains B1 and B2. The alkyl chains and graphene cores are well resolved in the images. Instead of the previous hexagonal honeycomb structure, a pseudohoneycomb structure is formed, as outlined in the images. From the adlayer symmetry and molecular orientation, unit cells for the assemblies in Fig. 4 *C* and *D* can be deduced. The parameters of the 2 unit cells are the same as $a = 2.60 \pm 0.1$ nm, $b = 3.05 \pm 0.1$ nm, and $\gamma = 75 \pm 2°$ with 4 molecules site at the corner and one inside the cell. Each unit cell includes 2 molecules. To clarify the molecular arrangement, 5 molecular models are superimposed in the images showing the relative positions of the molecules in the adlayer.

Domains B1 and B2 are mirror image to each other, showing a chiral symmetry. The structural models for the chiral packings are shown in Fig. 4 *F* and *G*. Enantiomorphic ordering in supramolecular assemblies by prochiral, or even achiral molecules have been reported (27–30). Upon adsorption of FTBC-C12 molecules on the achiral graphite surface, the domains with opposite chirality coexist across the whole surface and lead to local chirality.

STS Measurement. STS is used to study the electronic properties of FTBC on HOPG at ambient condition. Using the resonance between Fermi energy of the substrate and certain molecular orbitals of adsorbate when applying an appropriate bias on substrate, the value of highest occupied molecular orbital (HOMO), LUMO, and energy gap can be obtained from the I-V and dI/dV-V curve (31, 32). Fig. 5*A* shows the typical dI/dV-V curves of the ordered adlayers of FTBC-Cn (n = 4, 6, 8, 12). These curves are mostly overlapping, indicating similar electronic property. The edge defined by the cross-point of the tangents of the platform and uplift part of the curve represents the energy gap between HOMO and LUMO of FTBC-Cn. Large number of dI/dV-V curves are collected from each molecule to ensure accurate measurement of the energy gap. A representative histogram of FTBC-C6 is shown in Fig. 5*B*, showing the statistic distributions of the edges of HOMO and LUMO. The energy gap is then obtained by Gaussian simulation. DFT calculations were performed for isolated molecules of the 4 different species. The results show that both the HOMO and LUMO of FTBC-Cn (n = 4, 6, 8, 12) are mainly located on the π-conjugated cores of these graphene molecules.

Table 1 is a summary of the results from theoretical calculation and STS experiment. The calculated results from free FTBC-Cn molecules are close to the experimental data. All 4 molecules have almost the same energy gap, indicating that the alkyl chains have no significant influence on the electronic properties of the molecules.

Discussion

Up–Down Structure. An interesting alternating up–down structure is found in FTBC-C4 assembly shown in Fig. 2. The previous

Table 1. The theoretical and experimental results of HOMO, LUMO and energy gap of FTBC-Cn (n = 4, 6, 8, 12)

	FTBC-C4	FTBC-C6	FTBC-C8	FTBC-C12
Energy gap*, eV	2.41	2.43	2.44	2.49
HOMO†, ± 0.2 eV	−1.21	−1.19	−1.30	−1.28
LUMO†, ± 0.2 eV	1.18	1.22	1.15	1.16
Energy gap†, ± 0.4 eV	2.39	2.41	2.45	2.44

*Theoretical calculation results.
†the experimental results obtained by STS with STM probe.

results demonstrated that a Janus-type "double-concave" conformation is formed in the bulk crystal of this type of molecules according to the single-crystal X-ray diffraction data (25). However, the conformation of FTBC-Cn adsorbed on HOPG surface has not been reported, which might differ from the crystal phase due to the involvement of molecule-substrate interaction (19, 33). To understand the adsorption way on HOPG surface, DFT calculations were carried out for FTBC-C4 single molecule and assembly on HOPG. The theoretical results are shown in Fig. 6. Fig. 6 *A* and *C* show that an individual FTBC-C4 molecule has a planar conformation upon adsorption of HOPG. The driving force is the π-π interaction between the conjugated polycyclic aromatic core of the graphene molecule and HOPG. However, we constructed a FTBC-C4 assembly with the same unit cell as that in Fig. 2*C* on the HOPG surface. Fig. 6 *B* (top view) and *D* (side view) show the calculated results. It can be seen that the molecules on HOPG surface take 2 different orientations: (*i*) the conjugated core lies flat on HOPG, while the chains point upwards, and the molecules take an "up" orientation; (*ii*) alkyl chains adsorb on substrate and support the curved conjugated core, taking a "down" conformation. Based on this model we simulated the STM image of FTBC-C4 assembly (Fig. 6*E*), and it agrees well with the experimental results in Fig. 2*B*. In row A of Fig. 6*E* the molecules take "down" conformation and result in a bright contrast, while the molecules in row B take "up" conformation in a dark contrast.

Why do FTBC-C4 molecule take the same orientation in a row but opposite orientation in adjacent row during the self-

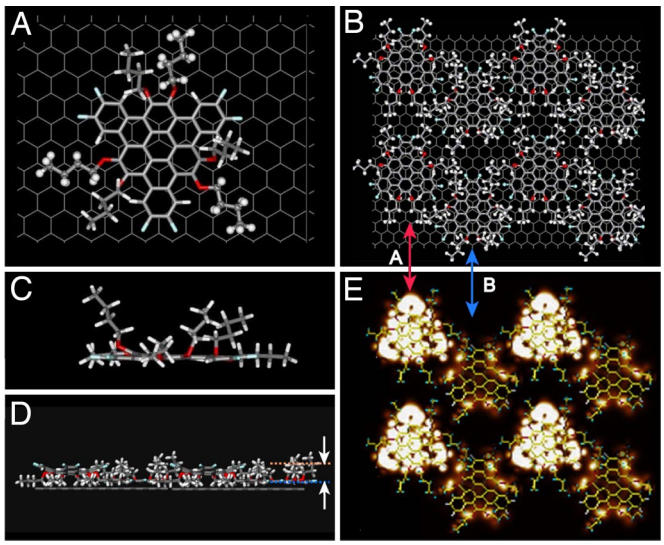

Fig. 6. The proposed model and theoretical simulation results for FTBC-C4 by DFT. (*A* and *B*) Top view of the optimized model of single molecule and periodic structure of monolayer on HOPG. Red (A) and blue (B) arrows indicate the "down" and "up" conformations respectively as in Fig. 2. (*C* and *D*) Side views of *A* (*C*) and *B* (*D*), respectively. (*E*) Simulation result of STM image on the base of *B*.

Table 2. Summary of structures and parameters of FTBC-Cn assemblies

	FTBC-C4	FTBC-C6	FTBC-C8	FTBC-C12	
Pattern	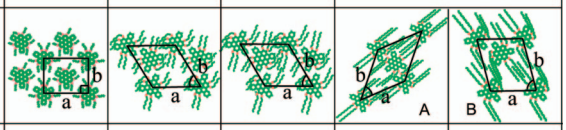				
a (± 0.1 nm)	2.62	2.60	2.70	2.78	2.60
b (± 0.1 nm)	2.12	2.60	2.70	3.20	3.05
Angle (± 2°)	90	60	60	45	75

assembly? The answer lies on the intermolecular interaction via C–H···F hydrogen bonds. As a relatively weak hydrogen bond, C–H···F plays a significant role in supramolecular chemistry. It was reported that the substitution of F atoms on benzene rings could strengthen the hydrogen bond (34–36). Van der Waals interaction between FTBC-C4 molecules in this arrangement is weak due to the lack of interdigitation of short alkyl chains. Therefore, hydrogen bonds play dominant role in the structure formation. The anisotropic C–H···F bonds direct FTBC-C4 molecules to self-organize into a close-packed assembly and help the molecules to maintain the curved conformation. As shown in Fig. 2*E*, the maximum distance of H···F bond is ≈0.254 nm and the minimum angle in C–H···F bond is 137°, consistent with the value reported in refs. 36–38.

Alkyl Chain Modulation. In general, the formation of a molecular self-assembly is governed by a delicate balance between intermolecular and molecule-substrate interactions. For FTBC-Cn molecules, the molecule-substrate interaction is originated from alkyl- and polycyclic aromatic core-substrate, while the intermolecular reaction is mainly from alkyl-alkyl (van der Waals force) and C–H···F hydrogen bonds. The molecule-substrate interaction drives the molecules to adsorb on the substrate through the conjugated core or alkyl chains. Intermolecular interactions makes the molecules form a close-packed adlayer to decrease the total energy in the system.

To understand the influence of alkyl chains on assembly structure, we increase the chain length from 4 to 6, 8, and 12 carbons. The resulted assembly patterns and parameters of the unit cells are listed in Table 2, summarizing the changes in the assembly structures with the alkyl chain length.

For FTBC-Cn (n = 6, 8, 12), the conformation of a single molecule on HOPG surface is similar to that of FTBC-C4. However, in an assembly, with the increase of alkyl chains, the van der Waals interaction between molecules and substrate becomes stronger and dominating factor (relative to the C–H···F hydrogen bond). As a result of the overall intermolecular and molecule-substrate interactions, the conformations of FTBC-Cn molecules adsorbed on HOPG surface vary from nonplanar (n = 4) to planar with longer alkyl chains (n = 6, 8, 12). In the latter case, all molecules take the same conformation and the conjugated curved cores of these molecules take planar conformation on HOPG surface.

As for the formation of honeycomb and lamellar structures, it is well known that aromatic molecules containing carboxyl functional groups, such as 1,3,5-benzenetricarboxylic acid and 1,3,5-tris-(carboxymethoxy)benzene are apt to form a hexagonal honeycomb structure via O–H···O hydrogen bonds (39). Hexagonal honeycomb structure has also been constructed by the molecules with long alkyl chains of 10 to 18 carbon atoms. The molecular assembly is usually formed through the chain interdigitation (24, 40). In this work, the weak C–H···F hydrogen bond is found to play an important role in forming the hexagonal lattice for FTBC-C6 and FTBC-C8. For FTBC-C12, 2 different patterns with lamellar and pseudohoneycomb structures, are observed. The lamellar structure is dominated by van der Waals interaction from the interdigitation of alkyl chains. The pseudohoneycomb structure could be related to the hexagonal honeycomb structures as discussed above and the differences are attributed to the longer alkyl chains, which can interdigitate and lead to planner conformation of the molecules.

Conclusion

The self-assembly of FTBC-Cn molecules with Janus-type double-concave conformation is fabricated on HOPG surface. The structural dependence of the self-assembly on molecular conformation and alkyl chain is investigated by STM experiments and DFT calculations. An alternating face reverse up–down way is found in FTBC-C4 assembly. With the increase of alkyl chain length, the assemblies form various adlayers with honeycomb, lamellar, and pseudohoneycomb (chiral) structures. The results demonstrate that the self-assembly with these featured double-concave graphene molecule is governed by the balance between hydrogen bonds and van der Waals interactions. The electronic property of the featured graphene molecules is preserved when they are adsorbed on solid surface.

Materials and Methods

Chemicals and Substrate. FTBC-Cn with n-carbon side chains (n = 4, 6, 8, 12) were prepared in 3 steps from readily accessible hexabutoxytriphenylene, as described in ref. 25. Toluene (analytic grade) was purchased from the Beijing Shunyi Chemical Factory. HOPG (quality ZYB) was from Digital Instruments.

Molecular Adlayers and STM Measurements. The adlayer was prepared by depositing a drop (≈ 2 μl) of toluene solution containing 10^{-4} M FTBC-Cn (n = 4, 6, 8, 12) onto freshly cleaved HOPG with an atomically flat surface. After evaporation of the solvent, the STM experiments were carried out in air with a NanoScope IIIa scanning probe microscope (Digital Instruments). The tunneling tips were prepared by mechanically cut Pt/Ir wire (90/10). All of the images were recorded in the constant-current mode. The specific tunneling parameters are given in the corresponding figure captions. The feedback of the STM control was turned off during STS measurements.

Calculation. Theoretical calculations were conducted using density functional theory as implemented in the DMol3 package. The Perdew–Burke–Ernzerhof function is used to describe exchange and correlation. All of the computations are all-electron, spin restricted, and performed with minimal basis set and medium integration mesh. The convergence thresholds for energy and electron density in self-consistent iterations are 1.0×10^{-5} a.u. and 1.0×10^{-3} a.u. for gradient and displacement in geometry optimizations. Simulated STM images were calculated by the Tersoff–Hamann approach, considering states above the Fermi level 750 meV. For extended systems, only the Γ point is considered.

ACKNOWLEDGMENTS. This work was supported by the National Natural Science Foundation of China Grants 20575070, 20673121, and 20733004; National Key Project on Basic Research Grants 2006CB806100 and 2006CB932100; and the Chinese Academy of Sciences.

1. Wallace PR (1947) The band theory of graphite. *Phys Rev* 71:622–634.
2. Novoselov KS, *et al.* (2004) Electric field effect in atomically thin carbon films. *Science* 306:666–669.
3. Meyer JC, *et al.* (2007) The structure of suspended graphene sheets. *Nature* 446:60–63.
4. Novoselov KS, *et al.* (2005) Two-dimensional atomic crystals. *Proc Natl Acad Sci USA* 102:10451–10453.
5. Wu J, Pisula W, Mullen K (2007) Graphenes as potential material for electronics. *Chem Rev* 107:718–747.
6. Li X, Wang X, Zhang L, Lee S, Dai H (2008) Chemically derived, ultrasmooth graphene nanoribbon semiconductors. *Science* 319:1229–1232.
7. Müllen K, Rabe JP (2008) Nanographenes as active components of single-molecule electronics and how a scanning tunneling microscopy puts them to work. *Acc Chem Res* 41:511–510.

8. Watson MD, Fechtenkotter A, Mullen K (2001) Big is beautiful-''aromaticity'' revisited from the viewpoint of macromolecular and supramolecular benzene chemistry. *Chem Rev* 101:1267–1300.
9. Samori P, Severin N, Simpson CD, Mullen K, Rabe JP (2002) Epitaxial composite layers of electron donors and acceptors from very large polycyclic aromatic hydrocarbons. *J Am Chem Soc* 124:9454–9457.
10. Iyer VS, *et al.* (1998) A soluble C60 graphite segment. *Angew Chem, Int Ed* 37:2696–2699.
11. Wang D, Wan LJ (2007) Electrochemical Scanning Tunneling Microscopy: Adlayer Structure and Reaction at Solid/liquid Interface. *J Phys Chem C* 111:16109–16130.
12. Wan LJ (2006) Fabricating and controlling molecular self-organization at solid surfaces: Studies by scanning tunneling microscopy. *Acc Chem Res* 39:334–342.
13. Li SS, *et al.* (2007) Control of supramolecular rectangle self-assembly with a molecular template. *J Am Chem Soc* 129:9268–9269.
14. Schock M, *et al.* (2006) Chiral close-packing of achiral star-shaped molecules on solid surfaces. *J Phys Chem B* 110:12835–12838.
15. Böhme T, Simpson CD, Müllen K, Rabe JP (2007) Current-voltage characteristics of a homologous series of polycyclic aromatic hydrocarbons. *Chem Eur J* 13:7349–7357.
16. Samori P, *et al.* (2001) Supramolecular staircase via self-assembly of disklike molecules at the solid-liquid interface. *J Am Chem Soc* 123:11462–11467.
17. Ito S, *et al.* (2000) Synthesis and self-assembly of functionalized hexa-peri-hexabenzocoronenes. *Chem Eur J* 6:4327–4342.
18. Wasserfallen D, *et al.* (2005) Influence of hydrogen bonds on the supramolecular order of hexa-peri-hexabenzocoronenes. *Adv Funct Mater* 15:1585–1594.
19. Ito S, *et al.* (2000) Bishexa-peri-hexabenzocoronenyl: A ''superbiphenyl.'' *J Am Chem Soc* 122:7698–7706.
20. Xiao SX, *et al.* (2005) Molecular wires from contorted aromatic compounds. *Angew Chem Int Ed* 44:7390–7394.
21. Hill JP, *et al.* (2004) Self-assembled hexa-peri-hexabenzocoronene graphitic nanotube. *Science* 304:1481–1483.
22. Wang ZH, Dotz F, Enkelmann V, Mullen K (2005) ''Double-concave'' graphene: Permethoxylated hexa-peri-hexabenzocoronene and its cocrystals with hexafluorobenzene and fullerene. *Angew Chem Int Ed* 44:1247–1250.
23. Hoeben FJM, Jonkheijm P, Meijer EW, Schenning APHJ (2005) About supramolecular assemblies of π-conjugated systems. *Chem Rev* 105:1491–1546.
24. Tahara K, *et al.* (2006) Two-dimensional porous molecular networks of dehydrobenzo[12]annulene derivatives via alkyl chain interdigitation. *J Am Chem Soc* 128:16613–16625.
25. Li Z, Lucas NT, Wang Z, Zhu D (2007) Facile synthesis of Janus ''double-concave'' tribenzo[a,g,m]coronenes. *J Org Chem* 72:3917–3920.
26. Chen Q, *et al.* (2008) STM investigation of the dependence of alkane and alkane (C18H38, C19H40) derivatives self-assembly on molecular chemical structure on HOPG surface. *Surf Sci* 602:1256–1266.
27. De Feyter S, *et al.* (1998) Expression of chirality by achiral coadsorbed molecules in chiral monolayers observed by STM. *Angew Chem Int Ed* 37:1223–1226.
28. Chen Q, Frankel DJ, Richardson NV (2002) Chemisorption induced chirality: Glycine on Cu{1 1 0}. *Surf Sci* 497:37–46.
29. Messina P, *et al.* (2002) Direct observation of chiral metal-organic complexes assembled on a Cu(100) surface. *J Am Chem Soc* 124:14000–14001.
30. Mamdouh W, *et al.* (2004) Expression of molecular chirality and two-dimensional supramolecular self-assembly of chiral, racemic, and achiral monodendrons at the liquid-solid interface. *Langmuir* 20:7678–7685.
31. Gong JR, *et al.* (2005) Direct evidence of molecular aggregation and degradation mechanism of organic light-emitting diodes under joule heating: An STM and photoluminescence study. *J Phys Chem B* 109:1675–1682.
32. Yang ZY, *et al.* (2007) Scanning tunneling microscopy of the formation, transformation, and property of oligothiophene self-organizations on graphite and gold surfaces. *Proc Natl Acad Sci USA* 104:3707–3712.
33. Constable EC, *et al.* (2006) An evaluation of the relationship between two- and three-dimensional packing in self-organised monolayers and bulk crystals of amphiphilic 2,2′: 6′,2″-terpyridines. *New J Chem* 30:1470–1479.
34. Zhang X, Yan CJ, Pan GB, Zhang RQ, Wan LJ (2007) Effect of C–H···F and O–H···O hydrogen bonding in forming self-assembled monolayers of BF2-substituted -dicarbonyl derivatives on HOPG: STM investigation. *J Phys Chem C* 111:13851–13854.
35. Desiraju GR (2002) Hydrogen bridges in crystal engineering: Interactions without borders. *Acc Chem Res* 35:565–573.
36. Thalladi VR, *et al.* (1998) C–H···F interactions in the crystal structures of some fluorobenzenes. *J Am Chem Soc* 120:8702–8710.
37. Oison V, Koudia M, Abel M, Porte L (2007) Influence of stress on hydrogen-bond formation in a halogenated phthalocyanine network. *Phys Rev B Condens Matter* 75:035428.
38. Rohde D, Yan CJ, Wan LJ (2006) C–H···F hydrogen bonding: The origin of the self-assemblies of bis(2,2′-difluoro-1,3,2-dioxaborine). *Langmuir* 22:4750–4757.
39. Yan HJ, Lu J, Wan LJ, Bai CL (2004) STM study of two-dimensional assemblies of tricarboxylic acid derivatives on Au(111). *J Phys Chem B* 108:11251–11255.
40. Shuhei Furukawa, *et al.* (2007) Structural transformation of a two-dimensional molecular network in response to selective guest inclusion. *Angew Chem Int Ed* 46:2831–2834.